APPLIED PHYSICS LETTERS VOLUME 74, NUMBER 2 11 JANUARY 1999

Picosecond ultrasonic study of Mo/Si multilayer structures using an alternating-pump technique

Nen-Wen Pu[a)] and Jeffrey Bokor
Department of Electrical Engineering and Computer Science, University of California, Berkeley, Berkeley, California 94720-1772

Seongtae Jeong
Center for X-ray Optics, Lawrence Berkeley National Laboratory, Berkeley, California 94720

Ri-An Zhao
Department of Material Science and Mineral Engineering, University of California, Berkeley, Berkeley, California 94720

(Received 7 August 1998; accepted for publication 12 November 1998)

We have used picosecond ultrasonics techniques to study the localized acoustic-phonon surface modes in Mo/Si multilayer reflectors for extreme ultraviolet lithography. Localized surface modes in the first (zone-boundary) and second (zone-center) gaps were simultaneously detected. Oscillation frequency as high as 0.873 THz was observed. An *alternating-pump* technique has been successfully demonstrated to enhance the signal-to-noise ratio by 10 dB. This technique can be used to improve the sensitivity for probing the surface modes in other multilayer thin-film structures. © *1999 American Institute of Physics.* [S0003-6951(99)03302-1]

Extreme ultraviolet (EUV) lithography is a promising candidate for the mass production of integrated circuits with design rules of 0.1 μm and below. The recent advances of multilayer mirrors which reflect EUV radiation have spurred great interest in projection lithography at EUV wavelengths. Mo/Si multilayers with reflectance of 67.5% at 13.4 nm are now routinely achieved.[1] The wavelength and value of the peak reflectance depend on the coating bilayer thickness d, and the value of Γ, defined as the thickness ratio of the Mo layer to the bilayer. Grazing incidence x-ray diffraction has been widely used in multilayer characterization because of its high accuracy in measuring the physical period d. However, it cannot accurately determine the Γ ratio. In addition, the small grazing angle requirement poses a difficulty when it comes to curved optics. Consequently, it is desirable to develop a characterization tool which can overcome these technical problems.

Picosecond ultrasonics has proven to be a useful technique for the study of the mechanical properties of thin films, multilayers, and other nanostructures. It is a pump-and-probe transient reflectivity technique in which the acoustic waves are impulsively excited by optical absorption of an ultrashort ''pump'' laser pulse and detected as a reflectivity change of the time-delayed ''probe'' laser beam. In particular, certain nonpropagating, persistent vibrations, named *localized surface modes* have been observed in several superlattices and multilayers,[2–6] and might be used to extract useful parameters of the structures. These modes may exist if the upper layer has the smallest acoustic impedance, and, for semi-infinite layers, vibrate at frequencies ν_{loc} (Refs. 2 and 3) such that

$$\tan\left(\frac{2\pi\nu_{\text{loc}}d_2}{c_2}\right)+\frac{\rho_1c_1}{\rho_2c_2}\tan\left(\frac{2\pi\nu_{\text{loc}}d_1}{c_1}\right)=0, \tag{1}$$

where d_1 and d_2 are the thicknesses, ρ_1,ρ_2 the densities, and c_1,c_2 the sound velocities of the top and bottom layers, respectively. These modes lie within the frequency band gaps of the dispersion curve and are localized within the topmost layers. It is evident from Eq. (1) that ν_{loc} is sensitive to both $d(=d_1+d_2)$ and Γ. The main difficulty for probing the surface modes is that the vibrational response of interest is, typically, 1–2 orders of magnitude weaker than an interfering electronic response of the materials, which itself is not large ($\Delta R_{\text{elec}}/R$ is usually on the order of 10^{-3}–10^{-6}).

In this letter, we report the successful application of this technique to the study of Si/Mo EUV multilayer mirrors. We have studied a series of multilayer structures in which the Γ ratio was 0.4 and the number of layers was 40. The bilayer thickness varies from 32.56 nm down to 6.84 nm, which is the typical thickness for practical EUV lithography optics. These d values were separately determined by small-angle x-ray diffraction with an accuracy within 0.1%. In the sample with the shortest period, vibration frequency as high as 0.873 THz was observed. Also, to significantly improve the signal-to-noise ratio, we propose and demonstrate an *alternating-pump* experimental technique.

The experimental configuration of this technique is shown schematically in Fig. 1. The light pulses were produced by a mode-locked Ti:sapphire laser operating at 800 nm, with a pulse duration of 120 fs and a repetition rate of 100 MHz. At this wavelength, the optical absorption occurs predominantly in Mo with an absorption length of ~20 nm. Both pump and probe beams were focused onto the sample with a spot size ~25 μm. An autobalanced detector circuit, which compares and balances the two inputs with an adjustable feedback-loop time constant, is used to help suppress low-frequency laser noise.

The main difference between this setup and the conventional pump–probe scheme is that two pumps, instead of one, were used to excite the sample. Pump beams A and B

[a)] Electronic mail: pun@eecs.berkeley.edu

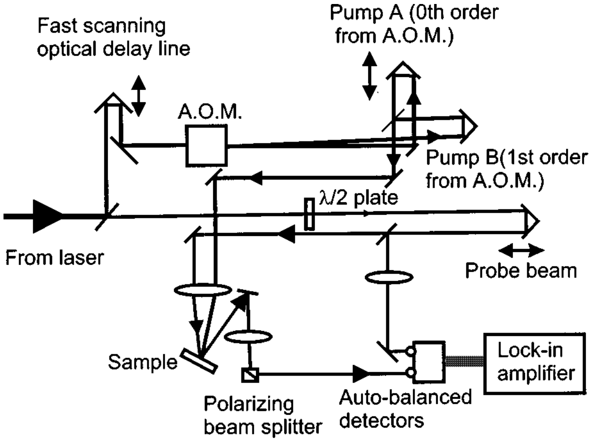

FIG. 1. Experimental setup (A.O.M.: acousto-optic modulator). Pumps A and B are, respectively, the zeroth- and the first-order diffracted beams from the A.O.M.

are, respectively, the zeroth- and the first-order diffracted beams from an acousto-optic modulator (diffraction efficiency ~90%), which is amplitude-modulated by a 100 kHz square wave. Thus, these two pumps come alternately onto the sample and the lock-in amplifier detects the difference of the responses excited by them. Figure 2 illustrates this idea: by adjusting the delay time τ_{AB} between pulses of pump A and pump B, relative to the probe pulse, it is possible to greatly suppress the slowly varying part of the large electronic response while the faster vibrational response is preserved. Figures 2(b) and 2(c) clearly show examples of near-perfect cancellation of the electronic response.

It is clear that two vibration modes were simultaneously excited in this sample. The difference between the traces in Figs. 2(b) and 2(c) is due to their different delay time: τ_{AB} is 0.57 and 1.14 ps for Figs. 2(b) and 2(c), respectively. In Fig. 2(b), τ_{AB} was set as one half of the period (0.57 ps) of the higher-frequency mode (~1/4 that of the lower-frequency mode), and thus, the higher-frequency mode was preferably revealed while the lower-frequency mode was slightly suppressed by a factor of $\sqrt{2}$. However, beating between these two modes is readily seen. By properly adjusting τ_{AB} to exactly one period (1.14 ps) of the higher-frequency mode, we successfully canceled this mode and clearly unveiled the other mode [Fig. 2(c)].

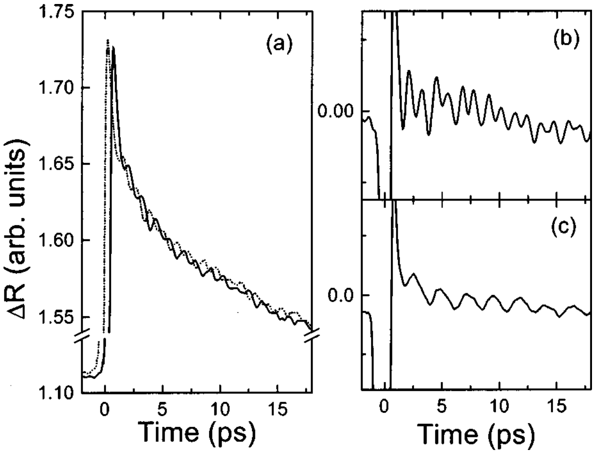

FIG. 2. Measurement of ΔR as a function of time for the Mo/Si multilayer ($d = 6.84\,\text{nm}$) using a conventional pump–probe technique (dotted line: with pump A only; solid line: with pump B only). (b) Same result obtained using the two-pump scheme with $\tau_{AB} = 0.57$ ps (second-gap mode fully revealed). (c) Two-pump scheme with $\tau_{AB} = 1.14$ ps (second-gap mode canceled).

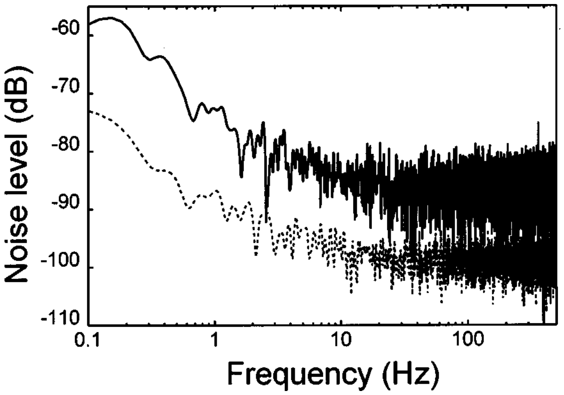

FIG. 3. Noise power spectra of the lock-in amplifier output at a fixed time delay $\tau_{AB} = 7$ ps using the conventional scheme (solid line) and the two-pump scheme (dashed line).

The primary advantage of this scheme is that the low-frequency noise of laser power fluctuations can be significantly suppressed. The reflected probe signal received by the detector is

$$P_{\text{sig}} = P_{\text{probe}}(t)[R + \Delta R(\tau)], \tag{2}$$

where $P_{\text{probe}}(t)$ is the probe beam power, R is the unperturbed reflectance, ΔR is the reflectance change induced by the pump, and τ is the delay time between pump and probe. $\Delta R(\tau)$ can be related to the pump power by $\Delta R(\tau) = P_{\text{pump}}(t-\tau)[\eta_{\text{elec}}(\tau) + \eta_{\text{vib}}(\tau)]$, where $\eta_{\text{elec}}(\tau)$ and $\eta_{\text{vib}}(\tau)$ are the electronic and vibrational responses, respectively. Considering the low-frequency fluctuation noise $n(t)$ of the laser power, $P_{\text{probe}}(t)$ can be written as $P_{\text{probe}}(t) = P_{\text{avg}} + n(t)$. Thus, we can rewrite Eq. (2) as

$$\begin{aligned} P_{\text{sig}}(t) &= [P_{\text{avg}} + n(t)]\{R + P_{\text{pump}}(t-\tau)[\eta_{\text{elec}}(\tau) \\ &\quad + \eta_{\text{vib}}(\tau)]\} = [P_{\text{avg}} + n(t)]R + \alpha[P_{\text{avg}} \\ &\quad + n(t)]^2 sw(\omega t)\,\eta_{\text{elec}}(\tau) + \alpha[P_{\text{avg}} \\ &\quad + n(t)]^2 sw(\omega t)\,\eta_{\text{vib}}(\tau), \end{aligned} \tag{3}$$

where we have assumed that $P_{\text{pump}}(t-\tau) = P_{\text{pump}}(t)$ since τ is negligible compared to the time scale of laser fluctuation, and that the pump is modulated with a square-wave form $sw(\omega t)$: $P_{\text{pump}}(t) = \alpha P_{\text{probe}}(t) \times sw(\omega t)$. The only term which contains the surface-mode information is the third term on the right-hand side of Eq. (3). The first term is eliminated by the balanced detectors. However, in the conventional pump–probe scheme, the second term, which manifests itself as the sharp rising edge and the slowly decaying tail in Fig. 2(a), passes through the balanced detectors and is amplified by the lock-in amplifier. Thus, the low-frequency fluctuation noise in this term (within the bandwidth of the low-pass filter in the lock-in amplifier) stays and becomes the primary noise source. In our two-pump scheme, this term is greatly suppressed and the last term dominates. Thus, the noise is suppressed by $\sim(\eta_{\text{elec}}/\eta_{\text{vib}})$ times, which is on the order of 10–100. Figure 3 shows the noise power spectrum of the lock-in amplifier output (at a fixed time delay τ

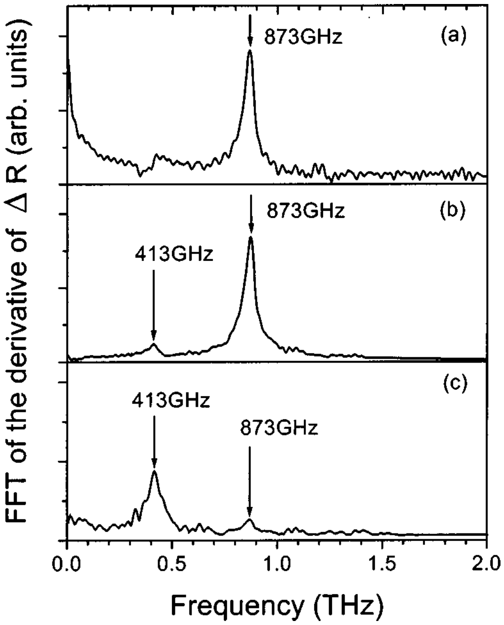

FIG. 4. Comparison of the fast Fourier transform of $d\Delta R(t)/dt$ using (a) the conventional scheme, (b) the two-pump scheme with $\tau_{AB}=0.57$ ps, and (c) $\tau_{AB}=1.14$ ps ($d=6.84$ nm).

$=7$ ps) spanning from 0.1 to 500 Hz. A 10–20 dB noise suppression throughout this frequency range was obtained by using the alternating-pump technique.

The relative delay between the probe and the pump beams was varied by a fast scanning optical delay line operating at 1.6 Hz and all of the traces in Fig. 2 were averaged 256 times. To further demonstrate the advantage of the alternating-pump technique, we took a trace using a conventional single-pump scheme (by blocking one of the two pumps) and compared the Fourier transform of the derivatives acquired using the two different methods (see Fig. 4). The ultrafast transient behavior in the first 2 ps was trimmed off before taking a Fourier transform to avoid a broadband background on the spectrum. It is evident that the spectra in Figs. 4(b) and 4(c) (two-pump scheme) are much cleaner than that in Fig. 4(a) (conventional scheme) and has a much lower dc component. In particular, the lower-frequency mode cannot be clearly discerned in Fig. 4(a), while in Fig. 4(b), it is undoubtedly observed, and in Fig. 4(c), by canceling the other mode, it is more explicitly revealed. These two vibration modes of frequencies at 413 and 873 GHz are the localized surface modes in the first (zone-boundary), and the second (zone-center) gaps, respectively. All of our samples show simultaneous presence of these two surface modes. The reason why the second-gap mode is stronger than the first-gap mode might be that, due to the spatial form of the initial stress or the sensitivity function, the latter is less strongly excited and/or detected.[3,4] The theoretical and measured values of the first- and second-gap surface-mode frequencies for all of our samples are listed in Table I. The measured frequencies of surface modes are inversely proportional to the bilayer thickness with an error of less than 5%. In addition, in all our samples the theoretical and experimental frequencies agree to within 20%. A possible origin of this discrepancy is the uncertainty of the density and sound velocity in the materials. (For the moment, we take the values for bulk materials: $\rho_{\mathrm{Si}}=2.33\,\mathrm{g/cm}^3$, $c_{\mathrm{Si}}=6.9\times10^5\,\mathrm{cm/s}$, $\rho_{\mathrm{Mo}}=10.22\,\mathrm{g/cm}^3$, and $c_{\mathrm{Mo}}=6.2\times10^5\,\mathrm{cm/s}$). Also, the silicide interlayers formed at Mo/Si interfaces smear the originally abrupt interfaces[7] and, thus, the assumption of perfectly abrupt interfaces in our calculation is unrealistic.

TABLE I. List of surface-mode frequencies in the first (zone-boundary) and second (zone-center) gaps determined by both theory ($\nu_{1\mathrm{th}}$ and $\nu_{2\mathrm{th}}$) and experiment ($\nu_{1\ \mathrm{exp}}$ and $\nu_{2\ \mathrm{exp}}$).

d (nm)	$\nu_{1\mathrm{th}}$ (GHz)	$\nu_{2\mathrm{th}}$ (GHz)	$\nu_{1\ \mathrm{exp}}$ (GHz)	$\nu_{2\ \mathrm{exp}}$ (GHz)
32.56	93	219	94	179
19.55	155	365	158	298
6.84	442	1043	413	873

In conclusion, we have excited and detected localized surface modes in Mo/Si multilayers using picosecond ultrasonics. An alternating-pump technique has been described and demonstrated to successfully separate the purely vibrational response of interest from the electronic response, and to significantly improve the signal-to-noise ratio. Modes in the first and second gaps have been simultaneously detected and a vibration frequency as high as 0.873 THz has been observed.

The authors thank Jim Underwood at the Center for X-ray Optics, Lawrence Berkeley National Laboratory, for providing the samples. This work is supported by the Semiconductor Research Corporation under Contract No. 96-LC-460, DARPA Advanced Lithography Program under Grant No. MDA972-97-0010, and AFOSR under Grant No. F49620-97-1-0220.

[1] C. Montcalm, S. Bajt, P. B. Mirkarimi, E. Spiller, F. J. Weber, and J. A. Folta, Proc. SPIE **3331**, 42 (1998).
[2] H. T. Grahn, H. J. Maris, and J. Tauc, Phys. Rev. B **38**, 6066 (1988).
[3] W. Chen, Y. Lu, H. J. Maris, and G. Xiao, Phys. Rev. B **50**, 14506 (1994).
[4] B. Perrin, B. Bonello, J. C. Jeannet, and E. Romatet, Physica B **219&220**, 681 (1996).
[5] B. Bonello, B. Perrin, E. Romatet, and J. C. Jeannet, Ultrasonics **35**, 223 (1997).
[6] H. T. Grahn, H. J. Maris, and J. Tauc, IEEE J. Quantum Electron. **25**, 2562 (1989).
[7] R. S. Rosen, D. G. Stearns, M. A. Viliardos, M. E. Kassner, S. P. Vernon, and Y. Cheng, Appl. Opt. **32**, 6975 (1993).